

# Effect of Nitrogen Content in Tunneling Dielectric on Cell Properties of 3-D NAND Flash Cells

Nagyong Choi, Ho-Jung Kang<sup>✉</sup>, Jong-Ho Bae<sup>✉</sup>, Byung-Gook Park<sup>✉</sup>, and Jong-Ho Lee<sup>✉</sup>, Fellow, IEEE

**Abstract**—The effect of band engineering by controlling nitrogen content in the tunneling dielectric of the 3-D NAND flash cells is investigated by comparing various cell properties of the two devices. These measured devices have the same device dimensions and different nitrogen contents. The device with higher nitrogen content shows larger trap density profile and improved erase characteristics. After the same P/E cycling stress, the device with higher nitrogen content shows larger increase of trap density and more significant degradation in its erase characteristics. The electrons stored in the device with higher nitrogen content more easily escape through the trap-assisted tunneling mechanism due to higher trap density, resulting in worse retention characteristics at room temperature.

**Index Terms**—3-D NAND flash memory, tunneling dielectric, band engineering, interface trap density.

## I. INTRODUCTION

RECENTLY, 3-D NAND flash memory with vertical bit-line (BL) has become a mainstream in the industry to obtain higher memory density and smaller bit cost [1]–[4]. In the structure based on bit-cost scalable (BiCS) technology, poly-Si body is separated from the substrate [4], so no holes can be supplied to the poly-Si body from the substrate during erase operation. So, Gate Induced Drain Leakage (GIDL) mechanism should be used to generate holes in the body in erase operation [5]. In order to improve erase characteristic without the structure change, band engineering can be applied to tunneling oxide [6], [7]. However, since the band engineering changes the dielectric property, it is necessary to study its effect on the cell characteristics. Previous studies about effects of band engineering have focused on hole/electron tunneling rate through the tunneling dielectric, program/erase (P/E)

Manuscript received February 12, 2019; accepted March 10, 2019. Date of publication March 15, 2019; date of current version April 25, 2019. This work was supported by the Brain Korea 21 Plus Project in 2018 and SK Hynix. The review of this letter was arranged by Editor D. Ha. (*Corresponding author: Jong-Ho Lee.*)

N. Choi, J.-H. Bae, B.-G. Park, and J.-H. Lee are with the School of Electrical and Computer Engineering, Seoul National University, Seoul 151-742, South Korea, and also with the Inter-University Semiconductor Research Center, Seoul National University, Seoul 151-742, South Korea (e-mail: jhl@snu.ac.kr).

H.-J. Kang is with the Research and Development Division, SK Hynix Inc., Icheon 467-701, South Korea.

Color versions of one or more of the figures in this letter are available online at <http://ieeexplore.ieee.org>.

Digital Object Identifier 10.1109/LED.2019.2905299

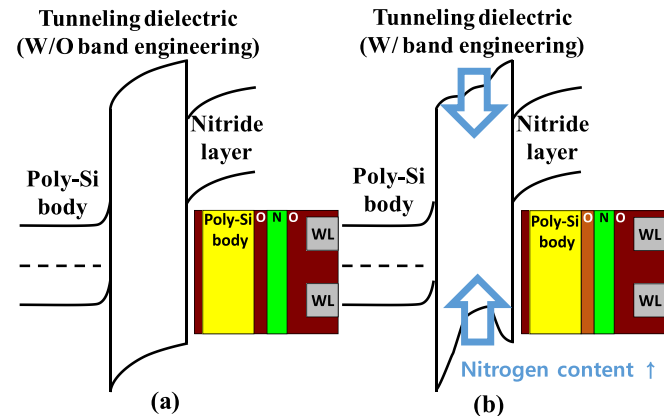


Fig. 1. Energy band diagrams along the WL direction of 3-D NAND flash memory cell, (a) without and (b) with band engineering in tunneling dielectric.

characteristics, gate leakage current, and oxide breakdown charge [6]–[10]. In particular, such studies have been mainly investigated in planar MOS devices, which have different channel material, device dimension, structure, and operation condition from those of 3-D NAND flash memory.

In this letter, we investigate the effect of the band engineering on the 3-D NAND flash memory cell properties. To compare the trap characteristics, we extract the trap density in wide-range of energy level from capacitance and conductance characteristics by utilizing conductance method [11], [12]. In order to analyze the effect of band engineering on the P/E characteristics, threshold voltage ( $V_{th}$ ) shift is observed with increasing step pulses. The effect of cycling stress on the cell characteristics is explained by comparing trap density profiles and P/E characteristics of the cells before and after the P/E cycling stress. At last, retention characteristics are compared.

## II. THEORY AND MEASUREMENT METHOD

Fig. 1 shows energy band diagrams of the 3-D NAND flash memory cells along the word-line (WL) direction without and with the band engineering. As shown in the Fig. 1 (b), band structure of the tunneling dielectric is changed by band engineering. This energy band change is more pronounced at the valence energy than at the conduction energy due to bandgap and affinity difference between oxide and nitride [6], [7]. The degree of the change becomes larger with increasing nitrogen content.

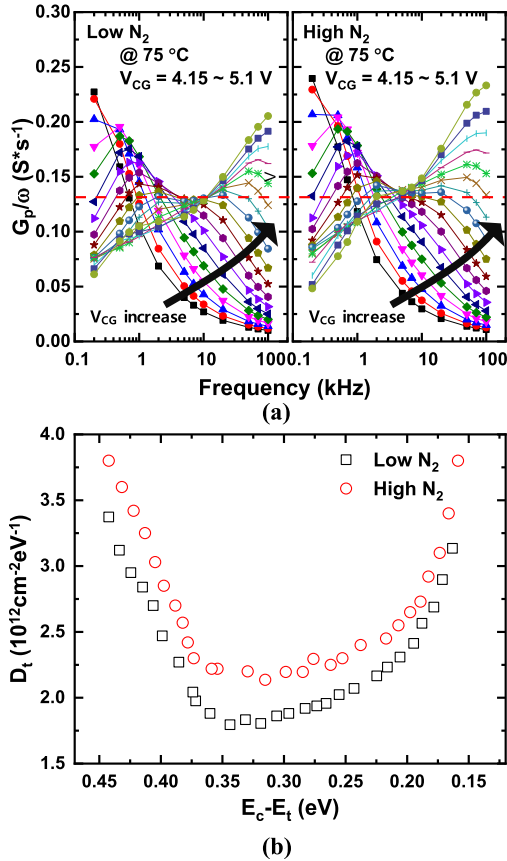


Fig. 2. (a)  $G_p/\omega$  curves of low and high  $N_2$  samples at 75 °C. (b) Extracted  $D_t$  profile of low and high  $N_2$  samples as a parameter of trap energy level.

In order to investigate the effect of the band engineering, we measured two 3-D NAND flash memory devices fabricated in the industry [3]. These two devices have the same device dimensions and fabrication process except  $N_2$  concentration in atmosphere during the tunneling dielectric fabrication process. These two devices are named low and high  $N_2$  samples, depending on nitrogen content.

### III. RESULTS AND DISCUSSION

#### A. Trap Characteristics

Fig. 2 shows parallel conductance over frequency ( $G_p/\omega$ ) curves and extracted trap density ( $D_t$ ) profiles of low and high  $N_2$  samples by utilizing conductance method [12]. As shown in Fig. 2 (a), peak values of  $G_p/\omega$  curves of high  $N_2$  sample at each control gate bias ( $V_{CG}$ ) are larger than that of low  $N_2$  sample. It results in higher  $D_t$  of the high  $N_2$  sample as in Fig. 2 (b). The  $D_t$  of the high  $N_2$  sample is about 18 % larger than that of the low  $N_2$  sample at energy level between 0.25 ~ 0.4 eV. This larger  $D_t$  in the high  $N_2$  sample is caused by excess nitrogen atoms which cause oxide internal stress and larger trap origins [13], [14].

During the P/E cycle, traps are generated due to repeated F-N tunneling [15]–[17]. After the 1k P/E cycles, these generated traps are observed as increased  $D_t$  as in Fig. 3. About 25 % and 47 % of  $D_t$  increase are observed in the low and high  $N_2$  samples. This larger trap generation of the high  $N_2$  sample with the same cycling stress is due to the greater mechanical stress in dielectric due to excess nitrogen atoms [13].

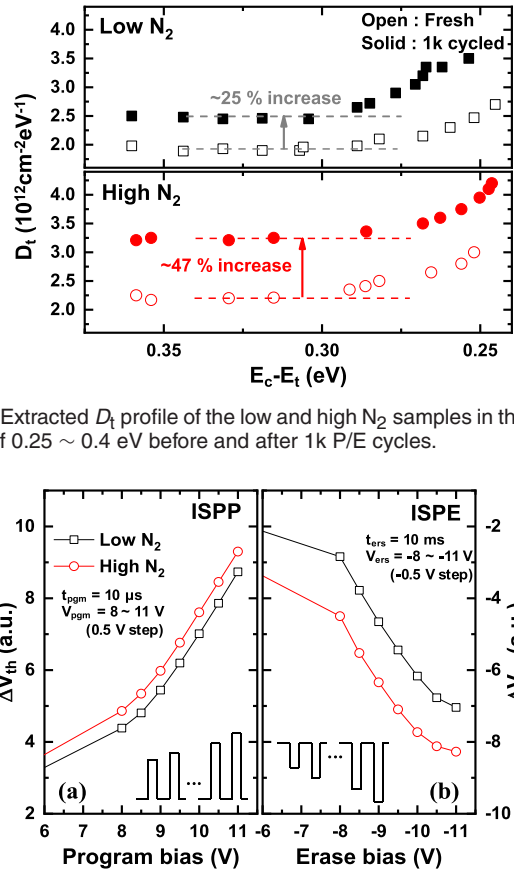


Fig. 3. Extracted  $D_t$  profile of the low and high  $N_2$  samples in the energy range of 0.25 ~ 0.4 eV before and after 1k P/E cycles.

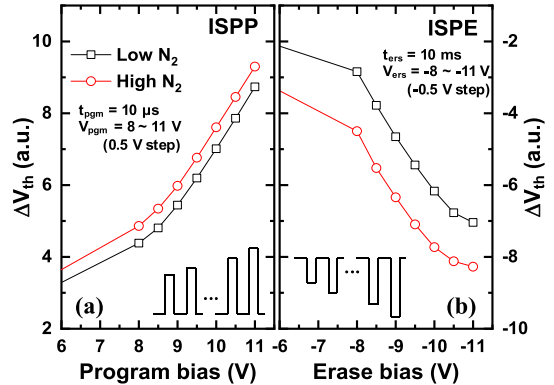


Fig. 4.  $\Delta V_{th}$  of low and high  $N_2$  samples by (a) ISPP and (b) ISPE. Insets show increasing step pulse waveform used in the measurements.

#### B. Program/Erase (P/E) Characteristics

Fig. 4 shows  $V_{th}$  shift ( $\Delta V_{th}$ ) by P/E biases with the increasing step (ISPP/ISPE). The insets show pulse waveform used in ISPP/ISPE. The high  $N_2$  sample shows larger  $\Delta V_{th}$  because the band offset during P/E operation is more significant in the high  $N_2$  sample due to larger band structure change. Moreover, since larger band offset occurs at valence band than at conduction band, erase characteristics shows larger improvement [6], [7]. Note that the slopes of ISPP/ISPE characteristics of the both samples are almost the same since the both samples are charge trap flash device [18].

Fig. 5 shows ISPP/ISPE characteristics of the two samples before and after 3k P/E cycles. In P/E cycling, the bias for one pulse is set to provide the same  $\Delta V_{th}$  in each sample. After the P/E cycles, P/E characteristics of the samples are changed due to buildup of trapped electrons in the devices [16]. In the ISPP measurement, both samples show about 4 % of  $\Delta V_{th}$  increase after the 3k P/E cycles. On the other hand, in the ISPE measurement,  $\Delta V_{th}$  of the low  $N_2$  sample shows about 9 % decrease after 3k P/E cycles while that of the high  $N_2$  sample shows about 15 % decrease. Larger deterioration in the erase operation of high  $N_2$  sample is due to the higher amount of trap generation and trapped electrons caused by excess nitrogen in the tunneling dielectric bulk [19], [20].

#### C. Retention Characteristics

Fig. 6 shows retention characteristics of the low and high  $N_2$  samples at 25 °C and 75 °C. The high  $N_2$  sample shows larger

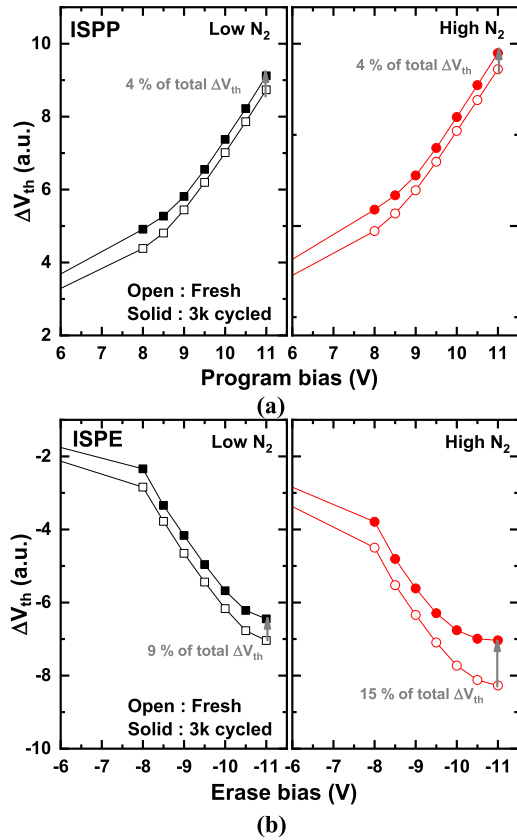


Fig. 5.  $\Delta V_{th}$  of low and high  $N_2$  samples by (a) ISPP and (b) ISPE, before and after 3k P/E cycles.

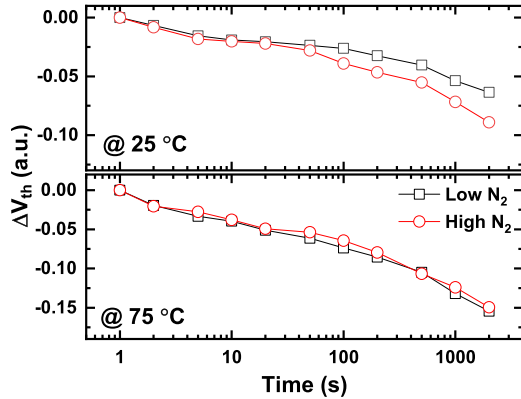


Fig. 6.  $V_{th}$  shift of low and high  $N_2$  samples at 25 °C and 75 °C for 2000 seconds.

$\Delta V_{th}$  at 25 °C than the low  $N_2$  sample while two samples show similar  $\Delta V_{th}$  at 75 °C. At 75 °C, electron escape by thermal emission mechanism is dominant so that effect of TAT can be ignored [21], [22]. Since the two samples have the same device dimensions and fabrication process except the nitrogen content in the tunneling dielectric, the amount of electrons escaped by thermal emission is similar, resulting in similar  $\Delta V_{th}$  at 75 °C. On the other hand, the effect of TAT term cannot be ignored at 25 °C and larger trap density in high  $N_2$  sample results in larger  $\Delta V_{th}$  at 25 °C.

#### IV. CONCLUSION

In this work, we have studied about effect of nitrogen content in tunneling dielectric on cell reliability of 3-D NAND

flash memory. The cell which has higher nitrogen content showed larger trap density and better erase characteristics compared to the cell with lower nitrogen content. When the same P/E cycling stress was applied to both samples, larger increase in trap density and a more severe erase characteristics degradation were observed in the cell with higher nitrogen content. In addition, it was shown from measured retention characteristics that a larger amount of electrons escapes from the storage layer of the cell with higher nitrogen content through the trap assisted tunneling mechanism. These results demonstrate that band engineering by controlling nitrogen content in the tunneling dielectric leads the advantage in erase characteristics but also leads poor P/E cycling endurance.

#### REFERENCES

- [1] Y. Fukuzumi, R. Katsumata, M. Kito, M. Kido, M. Sato, H. Tanaka, Y. Nagata, Y. Matsuoka, Y. Iwata, H. Aochi, and A. Nitayama, "Optimal integration and characteristics of vertical array devices for ultra-high density, bit-cost scalable flash memory," in *IEDM Tech. Dig.*, Dec. 2007, pp. 449–452. doi: [10.1109/IEDM.2007.4418970](https://doi.org/10.1109/IEDM.2007.4418970).
- [2] M.-K. Jeong, S.-M. Joe, H. Shin, B.-G. Park, and J.-H. Lee, "High-density three-dimensional stacked NAND flash with common gate structure and shield layer," *IEEE Trans. Electron Devices*, vol. 58, no. 12, pp. 4212–4218, Dec. 2011. doi: [10.1109/TED.2011.2168229](https://doi.org/10.1109/TED.2011.2168229).
- [3] S. K. Lee, S.-M. Ma, I. Seo, H. S. Shin, H. S. Kim, A. Cross, O. Baris, D. Kim, S. H. Lee, and S. Lange, "Investigation of novel inspection capability for 3D NAND device wordline inspection," in *Proc. 25th Annu. SEMI Adv. Semiconductor Manuf. Conf. (ASMC)*, May 2014, pp. 278–282. doi: [10.1109/ASMC.2014.6847021](https://doi.org/10.1109/ASMC.2014.6847021).
- [4] H.-J. Kang, M.-K. Jeong, S.-M. Joe, J.-H. Seo, S.-K. Park, S. H. Jin, B.-G. Park, and J.-H. Lee, "Effect of traps on transient bit-line current behavior in word-line stacked nand flash memory with poly-Si body," in *Symp. VLSI Technol. (VLSI-Technology), Dig. Tech. Papers*, Jun. 2014, pp. 1–2. doi: [10.1109/VLSIT.2014.6894348](https://doi.org/10.1109/VLSIT.2014.6894348).
- [5] Y. Komori, M. Kido, M. Kito, R. Katsumata, Y. Fukuzumi, H. Tanaka, Y. Nagata, M. Ishiduki, H. Aochi, and A. Nitayama, "Disturbless flash memory due to high boost efficiency on BiCS structure and optimal memory film stack for ultra high density storage device," in *IEDM Tech. Dig.*, Dec. 2008, pp. 1–4. doi: [10.1109/IEDM.2008.4796831](https://doi.org/10.1109/IEDM.2008.4796831).
- [6] H.-T. Lue, S.-Y. Wang, E.-K. Lai, Y.-H. Shih, S.-C. Lai, L.-W. Yang, K.-C. Chen, J. Ku, K.-Y. Hsieh, R. Liu, and C.-Y. Lu, "BE-SONOS: A bandgap engineered SONOS with excellent performance and reliability," in *IEDM Tech. Dig.*, Dec. 2005, pp. 547–550. doi: [10.1109/IEDM.2005.1609404](https://doi.org/10.1109/IEDM.2005.1609404).
- [7] H.-T. Lue, S.-C. Lai, T.-H. Hsu, P.-Y. Du, S.-Y. Wang, K.-Y. Hsieh, R. Liu, and C.-Y. Lu, "Modeling of barrier-engineered charge-trapping nandflash devices," *IEEE Trans. Device Mater. Rel.*, vol. 10, no. 2, pp. 222–232, Jun. 2010. doi: [10.1109/TDMR.2010.2041665](https://doi.org/10.1109/TDMR.2010.2041665).
- [8] C.-L. Cheng, K.-S. Chang-Liao, C.-H. Huang, and T.-K. Wang, "Current-conduction and charge trapping properties due to bulk nitrogen in  $HfO_xN_y$  gate dielectric of metal-oxide-semiconductor devices," *Appl. Phys. Lett.*, vol. 86, no. 21, Apr. 2005, Art. no. 212902. doi: [10.1063/1.1935768](https://doi.org/10.1063/1.1935768).
- [9] J. Ahn, W. Ting, and D.-L. Kwong, "Furnace nitridation of thermal  $SiO_2$  in pure  $N_2O$  ambient for ULSI MOS applications," *IEEE Electron Device Lett.*, vol. 13, no. 2, pp. 117–119, Feb. 1992. doi: [10.1109/55.144977](https://doi.org/10.1109/55.144977).
- [10] J.-S. Oh, S.-D. Yang, S.-Y. Lee, Y.-S. Kim, M.-H. Kang, S.-K. Lim, H.-D. Lee, and G.-W. Lee, "Tunneling oxide engineering by ion implantation of nitrogen for 3D vertical silicon pillar SONOS flash memory," *Microelectron. Eng.*, vol. 103, pp. 33–35, Mar. 2013. doi: [10.1016/j.mee.2012.08.005](https://doi.org/10.1016/j.mee.2012.08.005).
- [11] E. H. Nicollian and A. Goetzberger, "The si-sio, interface-electrical properties as determined by the metal-insulator-silicon conductance technique," *Bell Syst. Tech. J.*, vol. 46, no. 6, pp. 1005–1033, Jul./Aug. 1967. doi: [10.1002/j.1538-7305.1967.tb01727.x](https://doi.org/10.1002/j.1538-7305.1967.tb01727.x).
- [12] M.-K. Jeong, S.-M. Joe, B.-S. Jo, H.-J. Kang, J.-H. Bae, K.-R. Han, E. Choi, G. Cho, S.-K. Park, B.-G. Park, and J.-H. Lee, "Characterization of traps in 3-D stacked NAND flash memory devices with tube-type poly-Si channel structure," in *IEDM Tech. Dig.*, Dec. 2012, pp. 9.3.1–9.3.4. doi: [10.1109/IEDM.2012.6479010](https://doi.org/10.1109/IEDM.2012.6479010).

- [13] W. L. Hill, E. M. Vogel, V. Misra, P. K. McLarty, and J. J. Wortman, "Low-pressure rapid thermal chemical vapor deposition of oxynitride gate dielectrics for n-channel and p-channel MOSFETs," *IEEE Trans. Electron Devices*, vol. 43, no. 1, pp. 15–22, Jan. 1996. doi: [10.1109/16.477588](https://doi.org/10.1109/16.477588).
- [14] T. Arakawa, R. Matsumoto, and A. Kita, "Effect of nitrogen profile on tunnel oxynitride degradation with charge injection polarity," *Jpn. J. Appl. Phys.*, vol. 35, pp. 1491–1495, Feb. 1996. doi: [10.1143/JJAP.35.1491](https://doi.org/10.1143/JJAP.35.1491).
- [15] Y.-Y. Liao and S.-F. Horng, "The effects of program/erase cycles on the ONO stack layer in SONOS flash memory cell investigated by a variable-amplitude low-frequency charge-pumping technique," *IEEE Trans. Device Mater. Rel.*, vol. 9, no. 3, pp. 356–360, Sep. 2009. doi: [10.1109/TDMR.2009.2020992](https://doi.org/10.1109/TDMR.2009.2020992).
- [16] C. Sandhya, A. B. Oak, N. Chattar, U. Ganguly, C. Olsen, S. M. Seutter, L. Date, R. Hung, J. Vasi, and S. Mahapatra, "Study of P/E cycling endurance induced degradation in SANOS memories under NAND (FN/FN) operation," *IEEE Trans. Electron Devices*, vol. 57, no. 7, pp. 1548–1558, Jul. 2010. doi: [10.1109/TED.2010.2048404](https://doi.org/10.1109/TED.2010.2048404).
- [17] R. Micheloni, L. Crippa, and A. Marelli, *Inside NAND Flash Memories*. New York, NY, USA: Springer-Verlag, 2010, pp. 91–93.
- [18] H.-T. Lue, T.-H. Hsu, S.-Y. Wang, E.-K. Lai, K.-Y. Hsieh, R. Liu, and C.-Y. Lu, "Study of incremental step pulse programming (ISPP) and STI edge effect of BE-SONOS NAND flash," in *Proc. IEEE Int. Rel. Phys. Symp.*, Apr./May 2008, pp. 693–694. doi: [10.1109/RELPHY.2008.4558992](https://doi.org/10.1109/RELPHY.2008.4558992).
- [19] H. Meilin, X. Jingping, C. Jianxiong, and L. Lu, "Improved memory performance of metal-oxide-nitride-oxide-silicon by annealing the SiO<sub>2</sub> tunnel layer in different nitridation atmospheres," *J. Semicond.*, vol. 34, no. 11, Nov. 2013, Art. no. 114005. doi: [10.1088/1674-4926/34/11/114005](https://doi.org/10.1088/1674-4926/34/11/114005).
- [20] L.-H. Ko, B.-J. Cho, Y.-A. Nga, and L.-H. Chan, "The effect of nitrogen incorporation into the gate oxide by using shallow implantation of nitrogen and drive-in process," in *Proc. Hong Kong Electron Devices Meeting*, Aug. 1998, pp. 32–35. doi: [10.1109/HKEDM.1998.740182](https://doi.org/10.1109/HKEDM.1998.740182).
- [21] A. Arreghini, N. Akil, F. Driussi, D. Esseni, L. Selmi, and M. J. van Duuren, "Long term charge retention dynamics of SONOS cells," *Solid-State Electron.*, vol. 52, no. 9, pp. 1460–1466, Sep. 2008. doi: [10.1016/j.sse.2008.04.016](https://doi.org/10.1016/j.sse.2008.04.016).
- [22] A. Maconi, A. Arreghini, C. M. Compagnoni, G. van den bosch, A. S. Spinelli, J. van Houdt, and A. L. Lacaita, "Comprehensive investigation of the impact of lateral charge migration on retention performance of planar and 3D SONOS devices," *Solid-State Electron.*, vol. 74, pp. 64–70, Aug. 2012. doi: [10.1016/j.sse.2012.04.013](https://doi.org/10.1016/j.sse.2012.04.013).